Journal of Alloys and Compounds 501 (2010) 164–167

Contents lists available at ScienceDirect

Journal of Alloys and Compounds

journal homepage: www.elsevier.com/locate/jallcom

Fabrication of Al-based bulk metallic glass by mechanical alloying and vacuum hot consolidation

Xiu Wei [a], Fusheng Han [a,*], Xingfu Wang [a], Xinfu Wang [a], Cui'e Wen [b]

[a] Key Laboratory of Materials Physics, Institute of Solid State Physics, Chinese Academy of Sciences, Hefei 230031, China
[b] Center for Material and Fiber Innovation, Institute for Technology and Research Innovation, Deakin University, Pigdons Road, Geelong, Victoria 3217, Australia

ARTICLE INFO

Article history:
Received 9 February 2010
Received in revised form 3 April 2010
Accepted 7 April 2010
Available online 20 April 2010

Keywords:
Mechanical alloying
Bulk metallic glass
Al-based alloy
Vacuum hot pressing
Thermal stability

ABSTRACT

The $Al_{75}Ni_{10}Ti_{10}Zr_5$ bulk amorphous alloys have been synthesized by mechanical alloying and vacuum hot pressing. The as-milled powders and hot pressed samples were examined by X-ray diffraction, scanning electron microscopy, transmission electron microscopy, and differential scanning calorimetry. The $Al_{75}Ni_{10}Ti_{10}Zr_5$ amorphous powders with a high crystallization temperature of 790 K and a large supercooled liquid region of 49 K were prepared by ball milling elemental powder mixtures for 110 h. The bulk $Al_{75}Ni_{10}Ti_{10}Zr_5$ amorphous alloy was prepared by hot pressing at 733 K for 20 min under a pressure of 3 GPa. The Kissinger analysis indicated that the bulk metallic glasses exhibit high thermal stability. The Vickers microhardness of the bulk samples is in the range of 790–850 HV. The crack paths surrounding the indents of all these samples emanate from the indent corners, indicating that the propagation of cracks occurred by radiation.

1. Introduction

Bulk metallic glasses (BMGs) have attracted extensive interest for their excellent mechanical, physical and chemical properties. In particular BMGs exhibit unique mechanical properties including ultrahigh strength, high hardness, excellent wear, and corrosion resistance [1,2]. Since the first successful synthesis of an amorphous phase in an Au–Si system [3], a large number of BMGs based on different elements such as Zr, Fe, Cu, rear earth, Al and Mg have been obtained to date [4–7]. Among BMGs, Al-based amorphous alloys have attracted much attention because of their potential applications in the aerospace field due to their low density and high specific strength [8]. However, Al-based amorphous alloys are different from other conventional bulk metallic glasses. The glass formation range of Al-based alloys lies on the solute-rich side of the eutectic point where the liquidus temperature increases rapidly, resulting in a low reduced glass transition temperature, normally less than 0.5 [9]. Moreover, the atomic size criteria, normally employed for producing amorphous alloys, cannot be applied to the glass-forming ability (GFA) of Al-based amorphous alloys [10]. Due to their low GFA, the formation of Al-based metallic glasses by quenching is limited to dimension of thin ribbons (usually with a thickness < 100 μm), which evidently restricts their practical application. Mechanical alloying is an alternative way to synthesize amorphous composites compared with direct cooling from the melting metal liquid [11–15]. This is especially important for the alloy systems with low GFA in preparing amorphous powders and subsequently consolidating the amorphous powders into bulk samples with unlimited thickness and shape, using the viscous flow behavior in the supercooled liquid region [16–19]. In the present work, the synthesis and structure of the bulk $Al_{75}Ni_{10}Ti_{10}Zr_5$ amorphous alloys with a diameter of 10 mm and thickness of 2 mm were systemically studied. The thermal stability and the Vickers microhardness of the consolidated bulk amorphous alloy were also investigated.

2. Experimental

Elemental powders (99.9% purity) of Al, Ni, Ti, and Zr were weighted out to synthesize the amorphous alloy powder with a nominal composition (at.%) of $Al_{75}Ni_{10}Ti_{10}Zr_5$ by mechanical alloying (MA). The synthesis was performed in a planetary ball mill (QM-3SP4L) operated at 400 rpm using stainless steel vials and bearing steel balls (GCr15) with a ball to powder weight ratio of 20:1 in an argon atmosphere. The as-milled amorphous powders were consolidated in a vacuum hot pressing machine to produce bulk samples with a diameter of 10 mm and thickness of 2 mm, respectively. Hot pressing was conducted at 733 K for 20 min under a pressure of 3 GPa. The structures of as-milled powders and bulk samples were analyzed with X-ray diffraction (XRD) using Cu Kα radiation (X′ Pert Pro MPD), Scanning electron microscopy (SEM, FEI Sirion 200), and transmission electron microscopy (TEM, JEOL 2010), respectively. Thermal analysis was performed with differential scanning calorimetry (DSC, Pyris Diamond) at a constant heating rate under nitrogen atmosphere. The temperature axis as well as the enthalpy axis was calibrated using Indium and Zinc standards for all the heating rates. The Vickers microhardness of the bulk amorphous samples was measured using a machine under the load of 100, 200, 500, and 1000 g according to GB/T4340.1-1999 standard.

* Corresponding author. Tel.: +86 551 5591435; fax: +86 551 5591434.
E-mail address: fshan@issp.ac.cn (F. Han).

0925-8388/$ – see front matter © 2010 Elsevier B.V. All rights reserved.
doi:10.1016/j.jallcom.2010.04.069

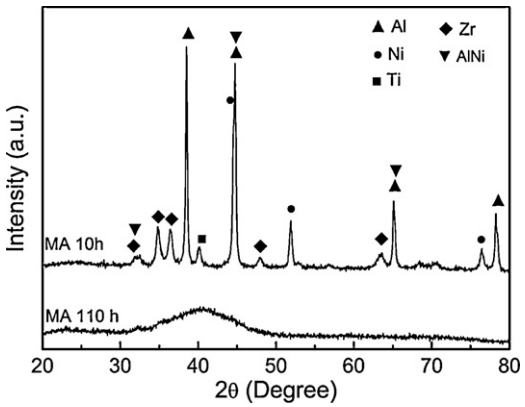

Fig. 1. XRD patterns of the $Al_{75}Ni_{10}Ti_{10}Zr_5$ powders milled for different times.

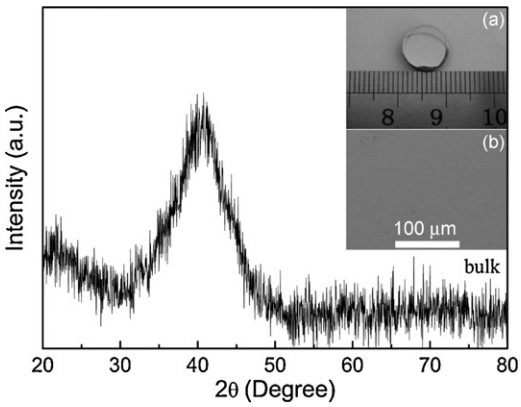

Fig. 3. XRD pattern for $Al_{75}Ni_{10}Ti_{10}Zr_5$ bulk disk sample. Inset (a) shows a camera photo of a disk with a diameter and thickness of 10 and 2 mm, respectively. The polished cross-sectional view of vacuum hot pressed $Al_{75}Ni_{10}Ti_{10}Zr_5$ disk sample was also shown in the inset (b).

3. Results and discussion

The XRD patterns of the starting and as-milled $Al_{75}Ni_{10}Ti_{10}Zr_5$ powders are shown in Fig. 1. The top curve shows the XRD pattern of a mixture of pure crystalline Al, Ni, Ti, and Zr milled for 10 h. It can be seen that when the peaks relating to the starting elements are excluded, some peaks indicating the compounds can be clearly observed. After milling for 110 h, all the crystalline peaks disappeared and only a broad diffraction peak existed, indicating that amorphization was completed.

The thermal stability of the $Al_{75}Ni_{10}Ti_{10}Zr_5$ amorphous powder was investigated by DSC. Fig. 2 shows the DSC curve of the 110 h as-milled $Al_{75}Ni_{10}Ti_{10}Zr_5$ amorphous powder at a heating rate of 20 K/min. It can be seen that the amorphous alloy powders exhibited an endothermic heat event of the glass transition followed by an obvious exothermic peak, further confirming the amorphous structure of the powders. The glass transition temperature (T_g, where T_g is the onset temperature of glass transition [20]), the onset of crystallization temperature (T_x^{onset}) and the peak crystallization temperature (T_x^{peak}) are determined to be 731.7, 780.6 and 797.9 K, respectively. The supercooled liquid region ΔT_x ($= T_x^{onset} - T_g$) is about 49 K. Compared to the other Al-based amorphous alloys [21], the $Al_{75}Ni_{10}Ti_{10}Zr_5$ amorphous powder exhibits a higher crystallization temperature and a wider supercooled liquid region, which could be attributed to the substitution of Zr for Al in the $Al_{80}Ni_{10}Ti_{10}$ amorphous alloys. In other words, the transition metal element addition substituting part of Al can improve the thermal stability of Al-based amorphous alloys.

Based on the DSC results, the as-milled powders after 110 h milling were consolidated into a disk shape with a diameter of 10 mm and a thickness of 2 mm, respectively. The powders were pressed under a pressure of 3 GPa for 20 min at 733 K. Fig. 3 shows the XRD pattern of the bulk sample of a hot pressed $Al_{75}Ni_{10}Ti_{10}Zr_5$ disk at 733 K. A morphology picture of the 10-mm-diameter amorphous disk is shown in inset (a) of Fig. 3. It can be seen that the sample exhibits a lustrous appearance which is typical for a bulk glassy alloy. The polished cross-sectional plane examined by the SEM is shown in inset (b) of Fig. 3, which indicates the bulk $Al_{75}Ni_{10}Ti_{10}Zr_5$ amorphous alloy with a highly dense structure has been prepared successfully. To confirm the phase nature of the bulk $Al_{75}Ni_{10}Ti_{10}Zr_5$ sample, the high-resolution TEM image and the inset selected-area electron diffraction (SAED) pattern are presented in Fig. 4. The sample was taken from the center of the bulk sample and exhibits a uniform microstructure with limited nanocrystallines in the high-resolution TEM image. The broad halo in the SAED pattern indicates the presence of a single amorphous phase, which coincides well with the XRD pattern showing that the sample is fully amorphous. It should be noted that the half-maximum line width for the halo pattern of the bulk sample in the XRD pattern is slightly narrower than that of the milled powder. This may be due to strain relief and limited nanocrystallization during the process of consolidation.

Fig. 5 shows the DSC curves of the bulk $Al_{75}Ni_{10}Ti_{10}Zr_5$ amorphous alloy sample at different heating rates. In all cases, a sharp

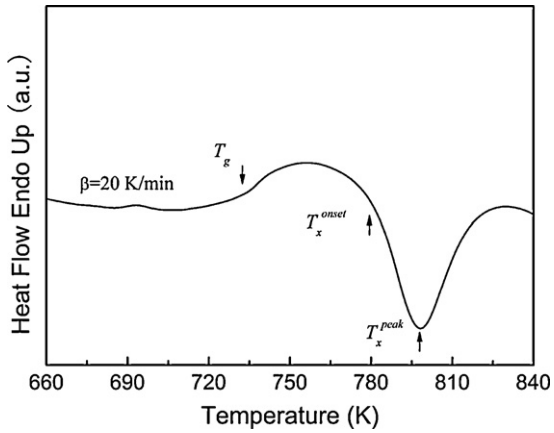

Fig. 2. The DSC curve of the $Al_{75}Ni_{10}Ti_{10}Zr_5$ amorphous powder at the heating rate of 20 K/min.

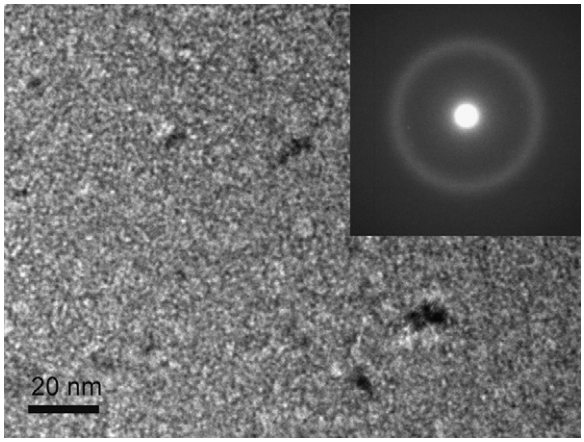

Fig. 4. High-resolution TEM images for the $Al_{75}Ni_{10}Ti_{10}Zr_5$ bulk disk samples. The inset shows the corresponding SAED pattern.

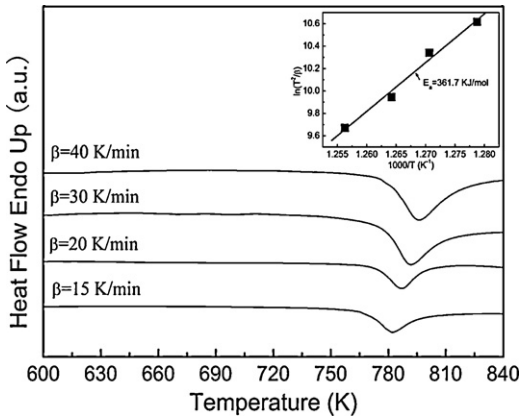

Fig. 5. DSC curves of the $Al_{75}Ni_{10}Ti_{10}Zr_5$ bulk disk sample at different heating rates, the Kissinger plot was shown in the inset.

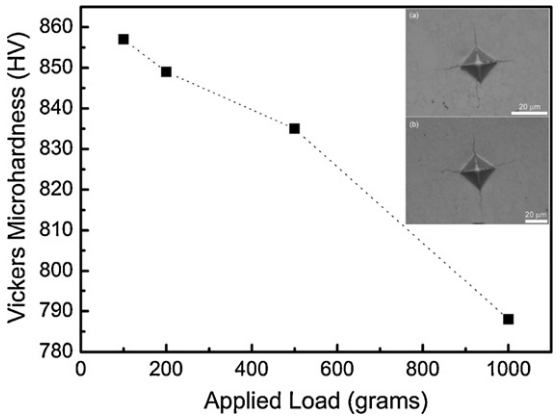

Fig. 6. The Vickers microhardness of the bulk $Al_{75}Ni_{10}Ti_{10}Zr_5$ amorphous disk tested at different indentation loads. The insets (a) and (b) show the Vickers microhardness indentation on the bulk $Al_{75}Ni_{10}Ti_{10}Zr_5$ amorphous disk sample with a load of 200 and 500 g, respectively.

exothermic crystallization peak is observed, but no significant endothermic event associated with the glass transition can be detected. These phenomena may be caused by the formation of some small fraction of crystallites in the process of consolidation, which are confirmed by the different half-maximum line width of the bulk and the amorphous powder. Upon heating the bulk sample with these pre-existing crystallites, crystallization ensues at T_g, which will essentially coincide with T_x. As a result, there is no obvious glass transition signal in the DSC curves. This phenomenon has also been illustrated by other researchers on the Al-based amorphous alloys [22–24]. The crystallization temperatures are listed in Table 1. In order to examine the thermal stability associated with crystallization kinetics of the bulk $Al_{75}Ni_{10}Ti_{10}Zr_5$ amorphous alloy, the $\ln(T^2/\beta)$ dependence of $1000/T_p$ is shown in the inset of Fig. 4 according to the relationship of Kissinger [25,26], where β and T_p are the heating rate and crystallization peak temperature, respectively. The slope corresponds to the effective activation energy for the crystallization (E_a) and exhibits a higher value of 361.7 kJ/mol than the other Al-based amorphous alloys. This implies that the bulk $Al_{75}Ni_{10}Ti_{10}Zr_5$ amorphous alloy has a high thermal stability.

The Vickers microhardness measurements were tested on the polished surfaces of the bulk amorphous disk samples (hot pressed at 733 K for 20 min). Fig. 6 shows the Vickers microhardness of the bulk amorphous disk samples tested at different indentation loads. As a result, the microhardness ranges from 788 to 857 HV which is larger than those of $Al_{70}Ni_{20}Ti_{10}$ and $Al_{85}Ni_{10}Zr_5$ metallic glass ribbons [27,28]. It should also be noted that the microhardness decreases visibly from 835 to 788 HV when the indentation load exceeds 500 g. The behavior in which the apparent hardness decreases with an increase in the applied load is similar to that observed in the conventional crystalline materials [29]. The change in the microhardness under different loads may be due mainly to the elastic response during the indentation. The relationship between the applied load and the indentation diagonal length follows the Meyer's law that fits more accurately when the applied load is relatively small [30]. For an idea indentation test, the microhardness is independent of the applied load. However, when the applied load is small, the elastic recovery relative to the indentation size is large and the residual deformation is small during the unloading. This may result in a relative high microhardness value of the materials when the load is small. Insets (a) and (b) in Fig. 6 show the Vickers microhardness indentation on the bulk $Al_{75}Ni_{10}Ti_{10}Zr_5$ amorphous disk sample with a load of 200 and 500 g, respectively. As the load is 200 g, limited small cracks from the indentation corners can be noticed. A further increase in the load to 500 g leads to the propagation and growth of the cracks. It should be noted that the crack paths surrounding the indents of all samples emanate from the indent corners, indicating that the propagation of cracks occurred by radiation.

Table 1
Kinetic parameters for the $Al_{75}Ni_{10}Ti_{10}Zr_5$ bulk amorphous alloy determined by non-isothermal analysis.

	β (K/min)			
	15	20	30	40
T_x^{onset} (K)	769	774	778	779
T_x^{peak} (K)	782	787	791	796

4. Conclusions

The $Al_{75}Ni_{10}Ti_{10}Zr_5$ amorphous powder alloys were successfully synthesized by mechanical alloying. The fully amorphous structure can be obtained after milling for 110 h. The as-milled $Al_{75}Ni_{10}Ti_{10}Zr_5$ amorphous powder exhibited a high crystallization temperature 790 K and a wide supercooled liquid region of 49 K. The as-milled amorphous alloy powders were subsequently consolidated successfully into bulk metallic glasses by vacuum hot pressing. The consolidation temperature was chosen in the supercooled liquid region. Limited nanocrystallines were noticed from XRD and DSC, which may result in no glass transition signals in the heating of bulk samples. The effective activation energy of crystallization is 361.7 kJ/mol, indicating a high thermal stability in the bulk metallic glass. The Vickers microhardness of the $Al_{75}Ni_{10}Ti_{10}Zr_5$ bulk samples is in the range of 790–850 HV. The crack paths surrounding the indents of all these samples emanate from the indent corners, indicating that the propagation of cracks occurred by radiation.

Acknowledgements

This work is supported by the National Basic Research Program of China in the No. 2006CB601201, the National Natural Science Foundation of China in the No. 50871107 and Science and Technology Program of Anhui Province, China, in the No. 07010302211.

References

[1] J. Schroers, W.L. Johnson, Phys. Rev. Lett. 93 (2004) 255506.
[2] A. Tauseef, N.H. Tariq, J.I. Akhter, B.A. Hasan, M. Mehmood, J. Alloys Compd. 489 (2010) 596–599.
[3] W. Klement, R.H. Willens, P. Duwez, Nature 187 (1960) 869–870.
[4] W.H. Wang, C. Dong, C.H. Shek, Mater. Sci. Eng. R 44 (2004) 45–89.

[5] A.H. Cai, W.K. An, Y. Luo, T.L. Li, X.S. Li, X. Xiong, Y. Liu, J. Alloys Compd. 490 (2010) 642–646.
[6] S. Bhattacharya, E.A. Lass, S.J. Poon, G.J. Shiflet, J. Alloys Compd. 488 (2009) 79–83.
[7] G.Q. Xie, D.V. Louzguine-Luzgin, Q.S. Zhang, W. Zhang, A. Inoue, J. Alloys Compd. 483 (2009) 24–27.
[8] L. Greer, Science 267 (1995) 1947–1953.
[9] Y. He, S.J. Poon, G.J. Shiflet, Science 241 (1988) 1640–1642.
[10] F.Q. Guo, S.J. Poon, G.J. Shiflet, Mater. Sci. Forum 31 (2000) 331–337.
[11] S. Scudino, S. Venkataraman, M. Stoica, K.B. Surreddi, S. Pauly, J. Das, J. Eckert, J. Alloys Compd. 483 (2009) 227–230.
[12] M. Seidel, J. Eckert, L. Schultz, J. Appl. Phys. 77 (1995) 5446–5448.
[13] G.H. Li, X.F. Bian, K.K. Song, J. Guo, X.L. Li, C.D. Wang, J. Alloys Compd. 471 (2009) L47–L50.
[14] D.K. Yang, C.E. Wen, F.S. Han, Y.J. Yang, J. Non-Cryst. Solids 352 (2006) 3244–3248.
[15] Y. Wang, X.X. Chen, H.R. Geng, Z.X. Yang, J. Alloys Compd. 474 (2009) 152–157.
[16] K.G. Prashanth, S. Scudino, B.S. Murty, J. Eckert, J. Alloys Compd. 477 (2009) 171–177.
[17] D.H. Bae, M.H. Lee, D.H. Kim, D.J. Sordelet, Appl. Phys. Lett. 83 (2003) 2312–2314.
[18] M.H. Lee, D.H. Bae, D.H. Kim, D.J. Sordelet, J. Mater. Res. 18 (2003) 2101–2108.
[19] K.B. Surreddi, S. Scudino, M. Sakaliyska, K.G. Prashanth, D.J. Sordelet, J. Eckert, J. Alloys Compd. 491 (2010) 137–142.
[20] Y.Z. Yue, J. Non-Cryst. Solids 354 (2008) 1112–1118.
[21] A. Samanta, I. Manna, P.P. CHattopadhyay, Mater. Sci. Eng. A 464 (2007) 306–314.
[22] K.K. Song, X.F. Bian, J. Guo, X.L. Li, M.T. Xie, C.J. Dong, J. Alloys Compd. 465 (2008) L7–L13.
[23] J.H. Perepezko, R.J. Hebert, R.I. Wu, G. Wilde, J. Non-Cryst. Solids 317 (2003) 52–61.
[24] D.V. Louzguine, A. Inoue, J. Non-Cryst. Solids 311 (2002) 281–293.
[25] H.E. Kissinger, Anal. Chem. 29 (1957) 1702–1706.
[26] H.E. Kissinger, J. Res. Natl. Bur. Stand 57 (1956) 217–221.
[27] A.P. Tsai, A. Inoue, T. Masumoto, Metall. Trans. 19A (1988) 1369–1370.
[28] A.P. Tsai, A. Inoue, T. Masumoto, J. Mater. Sci. Lett. 7 (1988) 805–807.
[29] P.M. Sargent, Microindentation Techniques in Materials Sciences and Engineering, ASTM STP 889, in: P.J. Blau, B.R. Lawn (Eds.), ASTM, Philadelphia, 1986. pp. 160–171.
[30] B.W. Mott, Microindentation Hardness Testing, Butterworths, London, 1956.